PROCEEDINGS OF SCIENCE

# Going beyond Top EFT

**André Lessa**[a,*] **and Veronica Sanz**[b]

[a] *Centro de Ciências Naturais e Humanas, Universidade Federal do ABC, Santo André, 09210-580 SP, Brazil*

[b] *Instituto de Física Corpuscular (IFIC), Universidad de Valencia-CSIC, E-46980 Valencia, Spain*

*E-mail:* andre.lessa@ufabc.edu.br, veronica.sanz@uv.es

We present a new approach for searching for new physics which bridges the gap between on-shell searches and effective field theories. Unlike the traditional Top EFT approach that focus on momentum distribution tails, we explore new physics effects emerging at loop-level, which can manifest as distinct structures on distributions at intermediate energy scales. We illustrate this with a UV model featuring a $\mathcal{Z}_2$ symmetry, incorporating a Dark Matter candidate and a top-partner. Considering the constraints from searches for the on-shell production of the top partner and from 1-loop effects to the top pair production, we illustrate the complementarity of both types of searches. We also compare the 1-loop results to the ones obtained using the EFT approximation and quantify how much it fails to capture the off-shell effects if the new physics scale is at a few TeV or below.

PoS(LHCP2024)316

*12th Large Hadron Collider Physics Conference (LHCP2024)*
*3-7 June 2024*
*Boston, USA*

*Speaker

## 1. Introduction

Despite the vast amount of results produced by the LHC experimental collaborations, no clear evidence for Beyond the Standard Model (BSM) physics has emerged so far. It is therefore extremely relevant to explore all approaches with potential to increase the LHC sensitivity to BSM scenarios. Currently two major approaches are employed when searching for new physics: i) searches for the on-shell production and decay of BSM states or ii) searches for off-shell effects from higher dimensional operators [1–7]. The latter often makes use of the Standard Model Effective Field Theory (SMEFT) framework [8], which is valid for new physics scales ($\Lambda$) beyond the the energy scales probed at the LHC ($\sqrt{s}$), i.e. $\Lambda \gg \sqrt{s} \sim O(\text{TeV})$.

The main goal of this paper is to bring forth a third way to interpret LHC measurements, namely to search for off-shell effects arising from new states which can be relatively light when compared to $\sqrt{s}$. Since in this case the EFT approximation is not valid, the off-shell contributions can not be described by the SMEFT operators. We will make use instead of form factors which can fully capture the off-shell effects from light BSM states. To illustrate this approach we will consider a top-philic BSM toy model and its effects to $t\bar{t}$ production at the LHC.

A comparison between the $t\bar{t}$ distributions using form factors or the corresponding EFT limit will allows us to properly quantify the regime under which the EFT approximation is valid and how much it fails to describe the effects of light ($\Lambda \lesssim \sqrt{s}$) new physics states. In addition we will show that the constraints from off-shell BSM effects on Standard Model (SM) observables can be competitive to on-shell searches for some regions of the parameter space. Finally, in Section 3 we will comment on possible improvements on search strategies which could enhance their sensitivity to BSM effects on SM measurements.

## 2. Top-Philic Toy Model

The possibility of new physics being primarily coupled to the top sector has been extensively studied in several BSM scenarios [9–12]. Here we consider a minimal toy model, which contains a scalar top partner ($\phi_T$), singlet under $SU(2)_L$, and a singlet Majorana fermion ($\chi$), which is a Dark Matter (DM) candidate. In addition we impose a $\mathcal{Z}_2$ symmetry under which the BSM fields are odd and the SM fields are even. The renormalizable BSM Lagrangian reads:

$$\mathcal{L}_{BSM} = \bar{\chi}\left(i\not{\partial} - \frac{1}{2}m_\chi\right)\chi + |D_\mu\phi_T|^2 - m_T^2|\phi_T|^2 - \left(y_{\rm DM}\phi_T^\dagger\bar{\chi}t_R + h.c.\right) \tag{1}$$

with $m_T > m_\chi$, so the DM candidate is stable. The $\phi_T$ field couples to the SM gluons, since it is colored and to the top quark and $\chi$ through the term proportional to $y_{\rm DM}$. The DM candidate on the other hand only couples through the latter. This scenario is similar to the minimal supersymmetric standard model (MSSM) with all the superpartners decoupled, except for the Bino and right-handed stop fields. Within the MSSM, however, we have $y_{\rm DM} = \frac{2\sqrt{2}}{3}g' \simeq 0.3$, where $g'$ is the $U(1)_Y$ coupling constant. In the scenario discussed here we assume $y_{DM}$ to be a free parameter, which can be as large as allowed by perturbativity, $y_{DM} \lesssim 4\pi$.

If $m_T \lesssim$ TeV, the scalar top partner will be abundantly produced at the LHC through the diagrams shown in Figure 1. The sensitivity to this process strongly depends on $\Delta M \equiv m_T - m_\chi$,

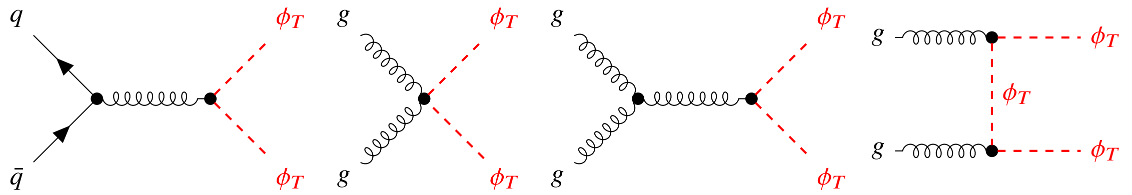


**Figure 1:** Leading order diagrams for the on-shell production of the colored scalar.

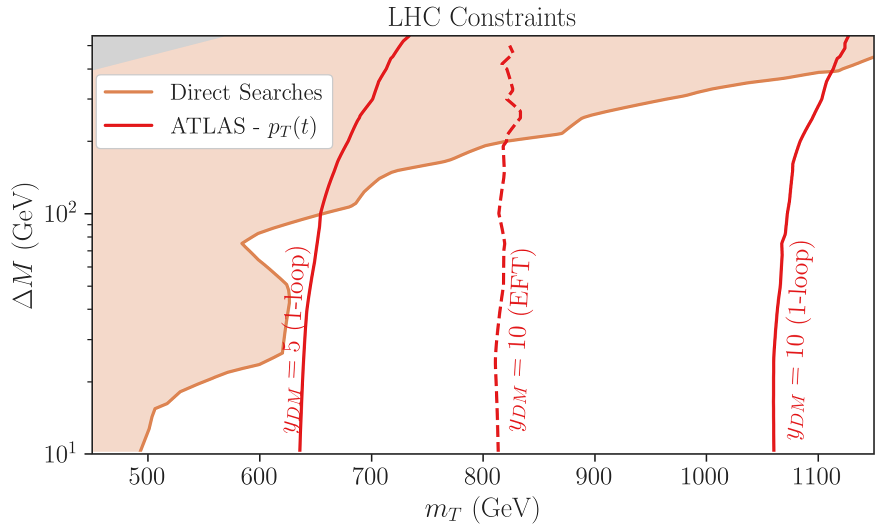


**Figure 2:** 95 % C.L. exclusions in the $m_T$ versus $\Delta M = m_T - m_\chi$ plane from direct searches (orange curve) and off-shell effects (red curves). The solid lines show the exclusion obtained using the full 1-loop calculation, while the dashed lines correspond to the EFT approximation for distinct values of the BSM coupling $y_{DM}$. The limits for the 1-loop and EFT curves were obtained using the ATLAS $p_T$ measurement from Ref. [18].

since for $\Delta M < m_t$, the $\phi_T$ decay will take place through an off-shell top ($\phi_T \to \chi + t^*(bff')$). Note, however, that the signal does not dependent on the BSM coupling $y_{DM}$, which only affects the scalar width.[1] Since LHC signatures for on-shell $\phi_T$ pair production are identical to the ones used for stop searches, we use SModelS [13–16] to reinterpret the ATLAS and CMS constraints on stop-neutralino simplified models and compute the constraints on the top-philic scenario considered here. For sufficiently small $\Delta M$, the signal can also be constrained by monojet searches, so we have recast the CMS monojet search [17] and used it to constrain the region with $\Delta M < 15$ GeV. The resulting 95% C.L. excluded region is shown by the orange curve in Figure 2.

From the above results we see that models with $m_T \gtrsim 1$ TeV and $\Delta M < m_t$ are still allowed by direct (on-shell) searches. Hence it is interesting to investigate if off-shell effects on $t\bar{t}$ production can be sufficiently large to be tested using top measurements. At 1-loop the $\phi_T$ and $\chi$ states contribute to $pp \to t\bar{t}$ as illustrated by the diagrams shown in Figure 3. Unlike the case of on-shell production, which is independent of $y_{\rm DM}$, the 1-loop contribution is proportional to $y^2_{\rm DM}$ and can be

[1] For the $y_{DM}$ values used in this work the width is sufficiently large to always result in prompt decays.

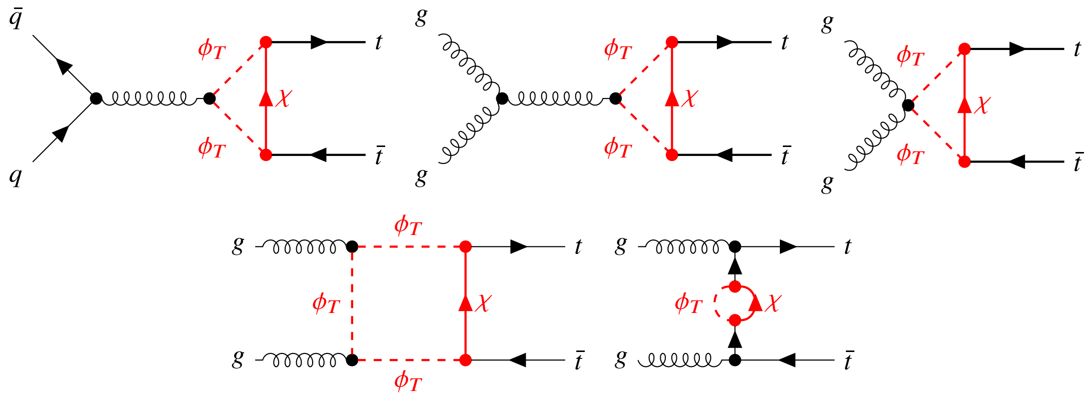


**Figure 3:** Examples of next-to-leading order BSM diagrams contributing to $pp \to t\bar{t}$. All the diagrams are of order $O(g_s^2 y_{\rm DM}^2)$.

enhanced for sufficiently large values of this coupling and/or small $m_T, m_\chi$. In order to compute the 1-loop contributions we have calculated form factors for the effective top-top-gluon and top-top-gluon-gluon couplings induced by the loop diagrams, which can be written as effective, momentum dependent couplings [19]:

$$\mathcal{L}_{FF} = \pi^2 g_s y_{DM}^2 G_\mu \bar{t} \left[\mathcal{F}^\mu \left(p_t, p_{\bar{t}}\right)\right] t + \pi^2 g_s^2 y_{DM}^2 G_\mu G_\nu \bar{t} \left[\mathcal{F}^{\mu\nu} \left(p_g, p_t, p_{\bar{t}}\right)\right] t \tag{2}$$

where the $\mathcal{F}^\mu$ and $\mathcal{F}^{\mu\nu}$ form factors contain the full momenta dependence as well as the Dirac and color structures, which are suppressed for simplicity.

In the EFT limit, i.e. $m_T, m_\chi \gg \sqrt{s}, m_t$, the 1-loop diagrams give rise to the following 6-dimensional operators:

$$\mathcal{L}_{EFT} = m_t C_g \, G^A_{\mu\nu} \left(\bar{t} T^A \sigma^{\mu\nu} t\right) + C_q \left(\bar{t}_R T^A \gamma^\mu t_R\right) \left(\bar{Q}_L T^A \gamma^\mu Q_L + \bar{u}_R T^A \gamma^\mu u_R + \bar{d}_R T^A \gamma^\mu d_R\right), \tag{3}$$

where $u, d, Q$ represent any light quark flavor and $m_t$ is the (on-shell) top mass. The Wilson coefficients $C_g$ and $C_q$ were computed using Matchete [20] and are given by:

$$C_g = -\frac{g_s y_{DM}^2}{384\pi^2} \frac{1}{m_T^2} \frac{1}{(1-x)^4} \left[1 - 6x + 3x^2 + 2x^3 - 6x^2 \log(x)\right] \tag{4}$$

$$C_q = \frac{g_s^2 y_{DM}^2}{576\pi^2} \frac{1}{m_T^2} \frac{1}{(1-x)^4} \left[2 - 9x + 18x^2 - 11x^3 + 6x^3 \log(x)\right], \tag{5}$$

where $x \equiv m_\chi^2 / m_T^2$.

Using the Lagrangian from Eq.(2) we can compute the BSM off-shell contributions to $t\bar{t}$ production and compare them to the ones obtained using the EFT approximation, given by Eq.(3). Since we are considering the leading BSM contributions, when computing $pp \to t\bar{t}$ we only include the Born (SM) and SM-BSM interference terms. Figure 4 shows the total $p_T(t)$ for two sets of BSM masses and $y_{DM}$. The filled blue histogram shows the SM only distribution, while the SM+BSM distribution obtained using the 1-loop (EFT) calculation is shown by the solid (dashed) red histogram. The distributions include the fiducial cuts considered by the ATLAS analysis from Ref.[18] and can be directly compared to the unfolded data, shown by the black points in Figure 4. The bottom panels display the ratio of each histogram to the observed data in each $p_T$ bin and the light blue band shows the measurement uncertainties ignoring correlations. The left plot shows the distribution for "light" BSM masses, where we see that the 1-loop distribution clearly differs from the EFT approximation for all bins above 500 GeV. Once we consider the distribution for heavier masses (right plot), we see that the EFT validity extends a bit further, up to $p_T \sim 700$ GeV. It is also interesting to note that in the light scenario (left plot) the EFT approximation overestimates the signal for the highest bin, while for the heavy scenario it severely underestimates it. Therefore, whether the EFT approximation is conservative (underestimates the signal) or aggressive (overestimates the signal) depends on the region of parameter space and the $p_T$ bins considered. Finally, we point out that the EFT underestimates the signal in intermediate bins in both light and heavy scenarios. Since these are the most sensitive to constrain the signal (due to their smaller uncertainties), the EFT approximation typically underestimates the constraints on the model.

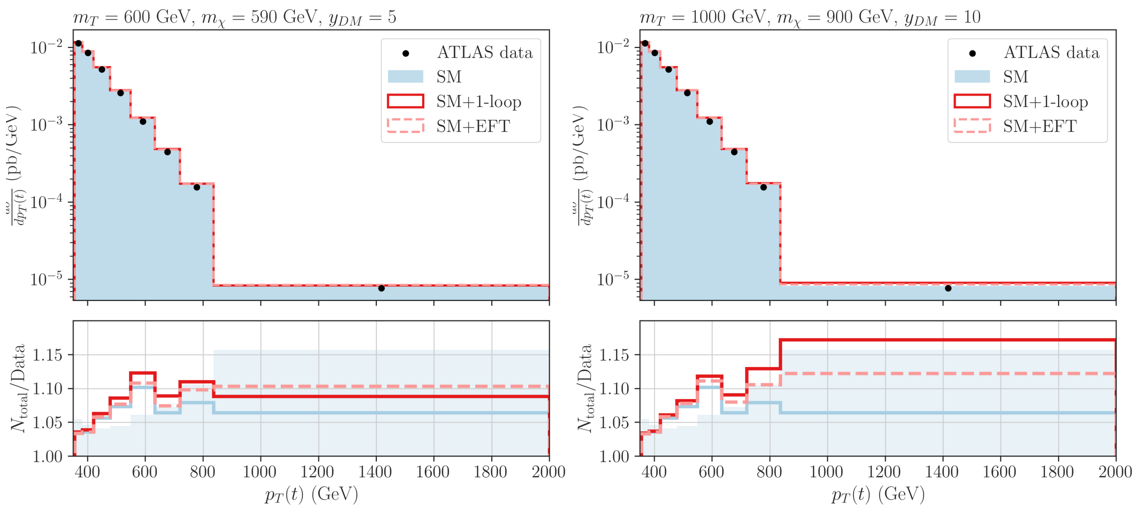


**Figure 4:** Transverse momentum distribution, $p_T(t)$, for $m_T = 600$ GeV, $m_\chi = 590$ GeV, $y_{DM} = 5$ (left) and $m_T = 1$ TeV, $m_\chi = 0.9$ TeV, $y_{\rm DM} = 10$ (right). The data points show the unfolded distribution measured by ATLAS [18], while the filled histogram shows the SM prediction at NNLO from Ref. [18]. The solid histogram shows the SM plus BSM distribution computed using the 1-loop form factors, while the dashed histogram shows the same distribution within the EFT approximation. The bottom subplot shows the ratio of the measured distribution to the SM, SM plus 1-loop and SM plus EFT distributions. The band shows the uncertainties ignoring correlations, i.e. $\sqrt{C_{ii}}$.

In Figure 2 we show the region excluded by the ATLAS $p_T(t)$ measurement at 95% C.L. for two values of $y_{\rm DM}$. The solid red curves show the excluded region using the 1-loop calculation, while the dashed curves show the region which would be obtained if we (wrongly) assumed the EFT approximation. As we can see, for $y_{\rm DM} = 5$, only the 1-loop results are competitive with direct searches, excluding $m_T \lesssim 650$ GeV for all $\Delta M$ values. For larger coupling values ($y_{\rm DM} = 10$), the exclusion extends up to 1 TeV. Furthermore, we see that the EFT approximation underestimates the sensitivity of top measurements to new physics.

## 3. Conclusions

In this paper, we discussed a new approach to reinterpret Standard Model top measurements, enabling to test scenarios with light new physics scales which can not be properly described by the SMEFT framework. We focused on scenarios that produce loop-induced signatures, motivated by Dark Matter. By computing the leading one-loop contributions to top pair production using effective couplings, we revealed that these BSM effects can differ significantly from the SMEFT operator behaviour. While Top EFT operators suggest an excess at the tails of distributions, our loop calculations resemble a broad bump. To fully capture new physics effects, it is essential to extend current SMEFT analyses and explore different kinematic regions beyond distribution tails. Our method shows that this reinterpretation is feasible using the same differential measurements, focusing on alternative phase space regions. In particular, the broad resonant signal behaviour and negative interference at high energy bins could be exploited further, particularly through ratios of intermediate and high invariant mass bins to reduce systematic uncertainties and enhance signal sensitivity. Leveraging these signal features enhances sensitivity to new physics beyond the typical SMEFT analyses. For sufficiently large BSM couplings, this sensitivity renders SM measurements complementary to direct searches, potentially extending the excluded BSM parameter space.

## References

[1] CMS collaboration, *Combined searches for the production of supersymmetric top quark partners in proton–proton collisions at* $\sqrt{s} = 13$ *TeV*, Eur. Phys. J. C **81** (2021) 970 [2107.10892].

[2] CMS collaboration, *Search for supersymmetry in proton-proton collisions at 13 TeV in final states with jets and missing transverse momentum*, JHEP **10** (2019) 244 [1908.04722].

[3] CMS collaboration, *Search for new physics in top quark production with additional leptons in the context of effective field theory using 138fb*$^{-1}$ *of proton-proton collisions at* $\sqrt{s} = 13$ *TeV*, Tech. Rep. CMS-PAS-TOP-22-006, CERN, Geneva (2023).

[4] CMS collaboration, *Search for new physics using effective field theory in 13 TeV pp collision events that contain a top quark pair and a boosted Z or Higgs boson*, Phys. Rev. D **108** (2023) 032008 [2208.12837].

[5] CMS collaboration, *Combined Higgs boson production and decay measurements with up to 137 fb-1 of proton-proton collision data at sqrts = 13 TeV*, Tech. Rep. CMS-PAS-HIG-19-005, CERN, Geneva (2020).

[6] CMS collaboration, *Measurement of* $W^{\pm}\gamma$ *differential cross sections in proton-proton collisions at* $\sqrt{s} = 13$ *TeV and effective field theory constraints*, Phys. Rev. D **105** (2022) 052003 [2111.13948].



PoS(LHCP2024)316

[7] ATLAS collaboration, *Top EFT summary plots September 2023*, Tech. Rep. ATL-PHYS-PUB-2023-027, CERN, Geneva (2023).

[8] B. Grzadkowski, M. Iskrzynski, M. Misiak and J. Rosiek, *Dimension-Six Terms in the Standard Model Lagrangian*, *JHEP* **10** (2010) 085 [1008.4884].

[9] U. Haisch and E. Re, *Simplified dark matter top-quark interactions at the LHC*, *JHEP* **06** (2015) 078 [1503.00691].

[10] T. Plehn, J. Thompson and S. Westhoff, *Dark Matter from Electroweak Single Top Production*, *Phys. Rev. D* **98** (2018) 015012 [1712.08065].

[11] A. Delgado, A. Martin and N. Raj, *Forbidden Dark Matter at the Weak Scale via the Top Portal*, *Phys. Rev. D* **95** (2017) 035002 [1608.05345].

[12] M. Garny, J. Heisig, M. Hufnagel and B. Lülf, *Top-philic dark matter within and beyond the WIMP paradigm*, *Phys. Rev. D* **97** (2018) 075002 [1802.00814].

[13] S. Kraml, S. Kulkarni, U. Laa, A. Lessa, W. Magerl, D. Proschofsky-Spindler et al., *SModelS: a tool for interpreting simplified-model results from the LHC and its application to supersymmetry*, *Eur. Phys. J. C* **74** (2014) 2868 [1312.4175].

[14] G. Alguero, S. Kraml and W. Waltenberger, *A SModelS interface for pyhf likelihoods*, *Comput. Phys. Commun.* **264** (2021) 107909 [2009.01809].

[15] G. Alguero, J. Heisig, C.K. Khosa, S. Kraml, S. Kulkarni, A. Lessa et al., *Constraining new physics with SModelS version 2*, *JHEP* **08** (2022) 068 [2112.00769].

[16] M. Mahdi Altakach, S. Kraml, A. Lessa, S. Narasimha, T. Pascal and W. Waltenberger, *SModelS v2.3: Enabling global likelihood analyses*, *SciPost Phys.* **15** (2023) 185 [2306.17676].

[17] CMS collaboration, *Search for new particles in events with energetic jets and large missing transverse momentum in proton-proton collisions at $\sqrt{s}$ = 13 TeV*, *JHEP* **11** (2021) 153 [2107.13021].

[18] ATLAS collaboration, *Measurements of differential cross-sections in top-quark pair events with a high transverse momentum top quark and limits on beyond the Standard Model contributions to top-quark pair production with the ATLAS detector at $\sqrt{s}$ = 13 TeV*, *JHEP* **06** (2022) 063 [2202.12134].

[19] A. Lessa and V. Sanz, *Going beyond Top EFT*, *JHEP* **04** (2024) 107 [2312.00670].

[20] J. Fuentes-Martín, M. König, J. Pagès, A.E. Thomsen and F. Wilsch, *A proof of concept for matchete: an automated tool for matching effective theories*, *Eur. Phys. J. C* **83** (2023) 662 [2212.04510].